Appl. Phys. A 90, 597–602 (2008)
DOI: 10.1007/s00339-007-4383-0

Applied Physics A
Materials Science & Processing

V. SKÁKALOVÁ[1,✉]
A.B. KAISER[1,2]
Z. OSVÁTH[3]
G. VÉRTESY[3]
L.P. BIRÓ[3]
S. ROTH[1]

Ion irradiation effects on conduction in single-wall carbon nanotube networks

[1] Max Planck Institute for Solid State Research, Heisenbergstr. 1, 70569 Stuttgart, Germany
[2] MacDiarmid Institute for Advanced Materials and Nanotechnology, SCPS, Victoria University of Wellington, P.O. Box 600, Wellington, New Zealand
[3] Research Institute for Technical Physics and Materials Science, Hungarian Academy of Sciences MFA, P.O. Box 49, 1525 Budapest, Hungary

Received: 3 August 2007 / Accepted: 14 December 2007
Published online: 4 January 2008 •

ABSTRACT We have measured how irradiation by Ar^+ and N^+ ions modifies electronic conduction in single-wall carbon nanotube (SWNT) networks, finding dramatically different effects for different thicknesses. For very thin transparent networks, ion irradiation increases localization of charge carriers and reduces the variable-range hopping conductivity, especially at low temperatures. However, for thick networks (SWNT paper) showing metallic conductivity, we find a relatively sharp peak in conductivity as a function of irradiation dose. Our investigation of this peak reveals the important role of thermal annealing extending beyond the range of the irradiating ions, and shows the dependence on the morphology of the samples. We propose a simple model that accounts for the temperature-dependent conductivity.

PACS 73.63.Fg; 61.80.-x

1 Introduction

Recently, the effect of defects on the conducting properties of individual metallic single-wall carbon nanotubes (SWNTs) was shown [1, 2] by the controlled reduction of the electronic localization length by irradiation with Ar^+ ions. For these SWNTs in the strong Anderson localization regime, the exponential increase of resistance with length of SWNTs between electrodes was greatly enhanced by di-vacancies created by the Ar^+ ions. In this paper, we report the first measurements (to our knowledge) of the effect of irradiation by ions on conduction in thin transparent SWNT networks, finding that resistance always increases on ion irradiation. In contrast to these results, however, we show that ion irradiation initially decreases the resistance of our thick SWNT networks.

Many applications proposed for carbon nanotubes [3–6] are likely to be sensitive to irradiation effects, which would be particularly significant, for example, for devices used in space or other high-radiation environments. Controlled irradiation also has many applications related to carbon nanotubes. It has been demonstrated by experimental and theoretical studies that irradiation can be used for nano-engineering of carbon nanotubes [7, 8]. For example, focused electron beams were shown to result in welding of crossed single-wall carbon nanotubes to form molecular junctions [9], and molecular dynamics simulations showed how such junctions might also be produced by irradiation by Ar^+ ions [10]. Irradiation by 1.25-MeV electrons at high temperature (800 °C) was able to coalesce neighbouring N-doped SWNTs as a result of defect formation followed by thermal annealing [11]. Using irradiation by Ar^+ ions, Stahl et al. [12] introduced defects in the SWNTs in the upper part of a bundle of loosely coupled SWNTs before depositing gold contacts on top of the bundle. They found that to avoid the defects, the current switched to undamaged nanotubes in the lower part of the bundle, tunnelling being the transfer mechanism between nanotubes.

In previous work [13], we observed local modifications of the electronic structure in atomically resolved scanning tunnelling microscope (STM) images of multi-wall carbon nanotubes after Ar^+ irradiation that were similar to those predicted [8, 14]. We also found that the defects tended to heal during annealing at the relatively moderate temperature of 450 °C for 90 min (the annealing was carried out in N_2 at a pressure of 5 bar).

For the case of thick SWNT networks with well-ordered bundles of nanotubes, metallic SWNTs dominate the conduction process and the conductance remains relatively large at helium temperatures [15]; we showed earlier [16, 17] that the temperature-dependent conductivity of our thick SWNT network samples agrees with that expected for quasi-one-dimensional (quasi-1D) metallic conduction interrupted by thin tunnelling barriers at defects.

We report here our observation of relatively sharp peaks in the conductivity of our thick SWNT network samples as a function of ion irradiation dose. We use Raman spectroscopy, measurements of temperature-dependent conductivity, and successive ion irradiation and direct heating experiments to show that heat propagation from ion impact sites to regions beyond the penetration depth of the ions plays a crucial role in producing these conductivity peaks. We found in earlier work [17] that as the thickness of SWNT networks is reduced, the conductance is no longer metallic but shows variable-range hopping (VRH)

✉ Fax: +49-711-689-1010, E-mail: v.skakalova@fkf.mpg.de

behaviour (with no conduction in the zero-temperature limit). In this case there are no conductivity peaks as the ion irradiation dose increases, only the strong reduction of conductance.

2 Experimental

Purified HiPCO SWNTs from Carbon Nanotechnologies, Inc. (Texas) were suspended in a 1% aqueous solution of sodium dodecyl sulfate (SDS) followed by ultra-sonication and centrifugation, and then air brushed onto quartz-glass plates. The sparse morphology of a typical very thin (transparent) SWNT network is illustrated in Fig. 1a, with SWNT bundles ranging from a few nm in height to more than 80 nm in some agglomerations (as shown by atomic force microscope (AFM) height profiles). Free-standing thick SWNT papers were prepared from a suspension of SWNTs in water with SDS by vacuum filtration. The surface morphology of a paper is illustrated in Fig. 1b. For ion irradiation of different doses, one of the papers was cut into several strips to ensure that the starting properties of the paper samples before irradiation were essentially identical.

The transparent SWNT films and strips of free-standing SWNT paper were introduced into an ion implanter and irradiated with Ar^+ ions and N^+ ions of energy 30 keV, using a dose from 0.5×10^{12} up to 25×10^{12} ions/cm^2 corresponding to exposures of 60–120 s respectively at ion current densities in the range of $J = 1$–60 nA/cm^2. The irradiation was done at normal incidence. After irradiation four parallel Pd/Au electrodes were evaporated on top of the SWNT transparent networks and free-standing papers and the electrical conductance was measured by the four-probe method from liquid-helium to room temperature. Raman spectra were measured using Raman spectroscopy at microscale resolution with a Jobin Yvon LabRam spectrometer with laser excitation wavelength 633 nm and spectral resolution 4 cm^{-1}.

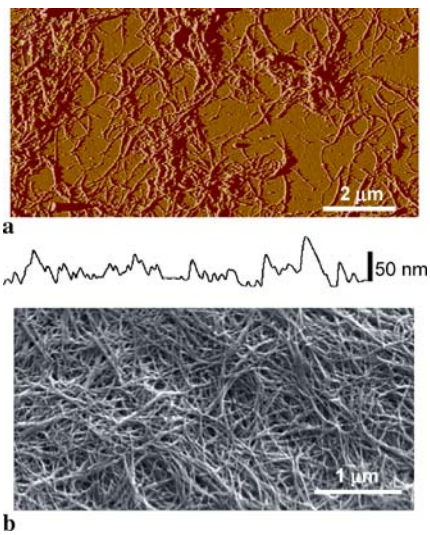

FIGURE 1 (**a**) AFM image of a SWNT transparent network, with a typical height profile *below* (the *vertical bar* corresponds to a height of 50 nm). (**b**) Scanning electron microscope (SEM) image of the surface of a free-standing SWNT paper

3 Penetration of the irradiating ions

We have simulated the penetration of ions of energy 30 keV into amorphous carbon with density 2.2 g/cm^3 using the TRIM code [18, 19], finding that Ar^+ ions penetrated approximately 50 nm and N^+ ions 80 nm deep into the carbon target, knocking a large number of carbon atoms from their atomic positions that then contributed to the irradiation damage. This indicates an average penetration depth approximately double these values for our SWNT paper of much lower density (1.2 g/cm^3). Additionally, the random networks of SWNTs contain a significant fraction of voids, in which the ions themselves and the knocked-out target atoms can move without losing energy. Therefore, both the penetration depth and the lateral spread of defects due to ion irradiation may be estimated as being 2 to 3 times larger than in the case of a bulk target.

To identify processes at different depths of the SWNT networks, we studied the transparent SWNT films with a height of up to 80 nm (that most ions pass right through) and free-standing 50-μm-thick papers of SWNTs (that stop all ions). For the thickness of 50 μm, only a small fraction of the total volume of the SWNT paper samples would be affected by direct collisions of the ions with carbon nanotubes (more accurate molecular dynamics simulations [8] would not change this general conclusion).

The D mode of the Raman spectra at 1302 cm^{-1}, which is characteristic

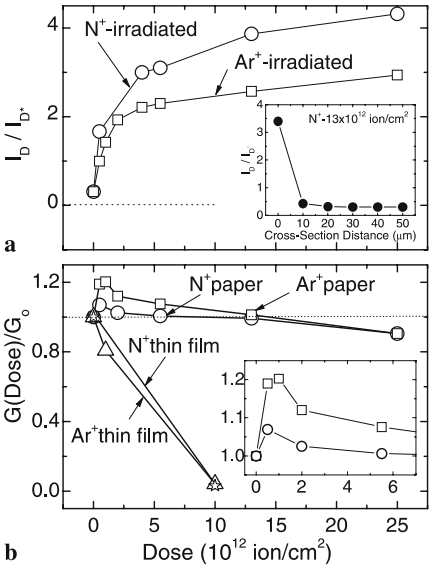

FIGURE 2 (**a**) Normalized intensities I_D/I_{D^*} of the Raman D to D^* lines for the SWNT paper samples as a function of Ar^+ and N^+ irradiation dose. *Inset*: the I_D/I_{D^*} ratios along the cross section from the irradiated side to the back side of the paper sample exposed to a dose of 13×10^{12} ions/cm^2 of N^+. (**b**) Conductivity at room temperature (normalized to its value before irradiation) for the transparent networks and the free-standing papers as a function of Ar^+ and N^+ irradiation dose. The *inset* shows the peaks in the conductance of the paper sample on a larger scale

of sp^3 bond defects in carbon nanotubes, increases strongly with irradiation, as shown in Fig. 2a by the plot of the D mode intensity I_D normalized by that of its second-order D^* mode that does not scale with defect concentration. However, the micro-Raman measurement along the cross section of the N^+-irradiated SWNT paper (inset to Fig. 2a) shows that, just a few μm below the irradiated surface of the SWNT paper, the normalized intensity I_D/I_{D^*} is almost unchanged from the value of the pristine sample. This confirms that ions do not penetrate far into the SWNT paper.

4 Effects of irradiation on conductivity

4.1 *Thin transparent SWNT films*

Our results for the effect of ion irradiation on the room-temperature sheet conductance of very thin transparent SWNT networks are shown in Fig. 2b. For these SWNT networks, only a reduction of conductance due to irradiation damage is observed. The temperature dependence plotted as $\log(G)$ vs. $T^{-1/2}$ (Fig. 3a) and lack of any

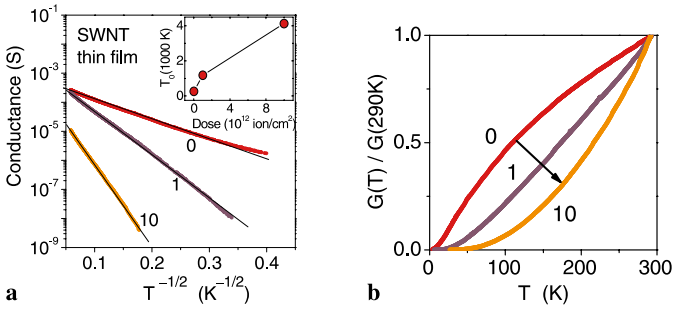

FIGURE 3 (**a**) Conductance G plotted as $\log(G)$ vs. $T^{-1/2}$ for our thin transparent film in the unirradiated state (labelled 0) and after Ar^+ irradiation doses of 1.0×10^{12} ions/cm^2 (labelled 1) and 10×10^{12} ions/cm^2 (labelled 10). The *inset* shows the dose dependence of the parameter T_0 calculated from (1). (**b**) The temperature dependence of the normalized conductance for the same three cases using linear scales, showing the suppression of conductance in the zero-temperature limit

conduction in the extrapolated zero-temperature limit of the curves of normalized conductance vs. temperature, presented in Fig. 3b, indicate that the overall conductance is limited by hopping conduction through disordered regions. The approximate linearity of the plot of $\log(G)$ vs. $T^{1/2}$ agrees with the variable-range hopping conductivity expression [20, 21]

$$\sigma(T) = \sigma_0 \exp\left(-\left(\frac{T_0}{T}\right)^{\gamma}\right), \qquad (1)$$

where the exponent $\gamma = 0.5$ is expected for one-dimensional variable-range hopping along SWNTs (but also for three-dimensional (3D) variable-range hopping taking account of electron–electron interactions [22]). The value of the parameter T_0 is inversely proportional to the cube of the localization length of the wavefunctions for the 3D case, and inversely proportional to the density of localized states at the Fermi energy [20]. The value of T_0 for our samples increases with irradiation dose (inset of Fig. 3a), indicating increasing localization of the wavefunctions due to irradiation. This localization of electrons at high-resistance points along the conduction paths is also reflected in the changing shape of the temperature dependence of the normalized conductance of the transparent SWNT films shown in Fig. 3b, with a much faster decrease of normalized conductance as temperature decreases for more localized electron states.

4.2 *Thick SWNT networks (SWNT paper)*

For our free-standing SWNT paper we find an initial sharp peak in conductivity (in contrast to the behaviour in the thin SWNT films), followed by a decrease with increasing irradiation dose, as shown in Fig. 2b. These results (to our knowledge) are the first observation of an increase in conductivity and a peak in conductivity as a function of ion irradiation in carbon nanotubes. Our group did find some evidence of an initial increase in conductivity (followed by a decrease) on gamma-ray irradiation of SWNT paper [23], and an increase in conductivity on irradiation (more plateau-like rather than a sharp peak) was seen for irradiation of SWNT bundles by ultraviolet light [24] and by high-energy electrons [25].

To understand the reasons for the very different behaviour of our SWNT paper samples compared to our very thin SWNT films, we have analysed in detail the temperature dependence of the conductivity of the SWNT papers (Fig. 4). We find (Fig. 4a) that the temperature dependence of the conductivity of the unirradiated SWNT paper follows very closely the expression for fluctuation-assisted tunnelling (FAT) through thin barriers between metallic regions [26]:

$$\sigma(T) = C \exp\left(-\frac{T_b}{T_s + T}\right), \qquad (2)$$

where C can be taken as a constant depending on the morphology of the samples. The order of magnitude of typical barrier energies is indicated by the value of $k_B T_b$ and the extent of the remaining conductivity at low temperatures is indicated by the ratio T_s/T_b. The fitted parameter values for the unirradiated sample are $T_b = 52$ K (4.5 meV) and $T_s/T_b = 0.37$. This behaviour is well known [21] for quasi-1D conductors such as conducting polymers or carbon nanotube networks with metallic regions separated by thin disordered conduction barriers.

From the plots in Fig. 4a for irradiated samples, we see that a key feature after irradiation is that the shape of the conductivity–temperature plot shows less tendency to saturation at higher temperatures and can no longer be accurately described by fluctuation-assisted tunnelling alone. However, the low-temperature behaviour remains clearly metallic with non-zero conductivity in the low-temperature limit, suggesting the continuing presence of fluctuation-assisted tunnelling between metallic regions. The stronger temperature dependence at higher temperature is sugges-

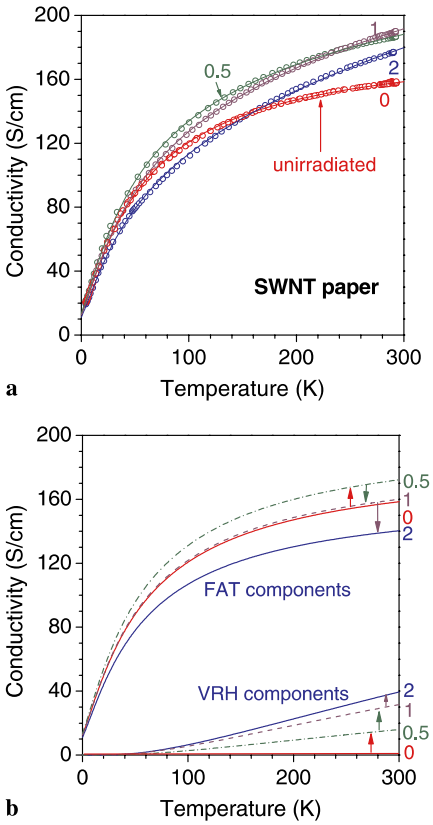

FIGURE 4 (**a**) Experimental data points of the conductivity of SWNT paper in its unirradiated state (*in red*) fitted to (2) for fluctuation-assisted tunnelling alone, and after Ar^+ irradiation (doses labelled beside each data set as 0.5 (*in green*), 1 (*in purple*), and 2 (*in blue*) in units of 10^{12} ions/cm^2) fitted to (3) with $\gamma = 0.5$ as discussed in the text. (**b**) The fitting curves to the data shown in (**a**) separated into the two components corresponding to the two terms in (3): the variable-range hopping (VRH) components and the fluctuation-assisted tunnelling (FAT) components. The *arrows* show the changes as irradiation dose increases (VRH terms systematically increase while FAT terms show, first, an increase and, then, a decrease)

tive of thermally activated or hopping conduction. We find that a very good description of the conductivity data is given by fluctuation-assisted tunnelling in parallel with hopping or activated conduction:

$$\sigma(T) = C \exp\left(-\frac{T_b}{T_s + T}\right) + H \exp\left(-\left(\frac{T_0}{T}\right)^{\gamma}\right), \quad (3)$$

as shown by the fits for the irradiated samples in Fig. 4a. In these fits the tunnelling parameters T_s and T_b are taken as unchanged from those for the pristine sample and only the magnitude of the tunnelling conductivity is varied. Since the hopping term is relatively small, the fit is good for different values of γ corresponding to hopping of different dimensionalities or activated conduction ($\gamma = 1$); we have taken $\gamma = 0.5$ for these fits.

The magnitude of the hopping and tunnelling components in the fits in Fig. 4a is plotted in Fig. 4b. The fraction of room-temperature conductivity contributed by the hopping term increases from zero in the pristine sample to approximately 20% for a dose of 2×10^{12} Ar^+ ions/cm^2. This identifies the hopping term that changes the shape of the conductivity temperature dependence as directly associated with the irradiation dose.

The fluctuation-assisted tunnelling term increases for the lowest dose of 0.5×10^{12} Ar^+ ions/cm^2, but drops back to a value very close to the pristine sample for a dose of 1.0×10^{12} Ar^+ ions/cm^2, and continues decreasing for the higher dose of 2×10^{12} Ar^+ ions/cm^2 (although the total conductivity is still larger than the initial conductivity). This initial increase of the metallic tunnelling conductivity indicates that after irradiation the nature of the tunnelling barriers has not been greatly altered, but the number of barriers has been reduced. Such barriers arise from defects along individual nanotubes, and intertube and inter-rope contacts, which are affected by adsorbed molecules and residual impurities. Improved alignment of SWNTs within bundles as small defects are eliminated would yield a substantial improvement in conductivity.

5 Origin of the conductivity peaks in SWNT paper

A possible cause of this removal of defect barriers, impurities, adsorbed molecules, or residues in irradiated SWNT paper is thermal annealing by the heat released by the collisions of the irradiating ions and target atoms knocked out by the incoming ions (our group recently investigated [27] the annealing of tunnelling barriers between a SWNT and a metal electrode by Joule heating due to a current pulse). As mentioned in the Introduction, significant healing of irradiation-induced defects by annealing at 450 °C was observed in multi-wall carbon nanotubes [13], and lesser temperatures are likely to affect the resistance due to desorption of impurities from intertube contacts or improved alignment of nanotubes within a bundle. Our TRIM simulation for irradiation of a bulk target indicates that a 30-keV Ar^+ ion transfers 800 eV/ion/nm to carbon atoms lying between the surface and a depth of 20 nm. For a (10,10) nanotube, and using [28] $c_v = 600$ J/kg K for the specific heat of SWNTs, this means that an Ar^+ ion would heat a 13-nm portion of a nanotube to a temperature of 500 °C. Such temperatures are sufficient to cause substantial annealing of defects and desorption of adsorbed impurities. It is clear that propagation of heat further into the sample (beyond the stopping range of the ions) would raise temperatures sufficiently for annealing effects considerably deeper than the penetration depth of the ions, depending on the heat conductivity and other factors.

Another possible cause of a conductivity increase on irradiation is the formation of covalent-bond cross-links between neighbouring SWNTS by carbon atoms displaced by the ions [25]. Cross-links would be associated with defects in the SWNT structure and therefore cause a decrease in the conductance of a previously defect-free SWNT. On the other hand, the conductance of a bundle of SWNTs could be increased by cross-links assisting transfer between SWNTs and reducing the separation of SWNTs. This effect, however, would be confined to the surface layers of the SWNT where ion impacts occur, so there would need to be a huge increase in conductivity in the ion impact layer of a few hundred nm to give the observed 20% rise in overall conductivity in our 50-μm-thick SWNT paper. In this case, one would expect a similar conductivity increase in the SWNT bundles in our thin SWNT films, where the impacts occur throughout the sample. But this is opposite to what we observe – there is a strong decrease in conductivity in the thin SWNT films. Hence, a model of enhanced conductivity beyond the impact region of the ions due to heat propagation is a more plausible explanation of the conductivity peaks in the SWNT paper. Note that the ions go through the SWNT thin films, depositing most of their heat energy in the substrate, while essentially all their energy appears as heat in the SWNT paper.

We propose that the origin of the conductivity peaks as a function of irradiation dose in the SWNT paper is as follows. The heat energy released by the ion and displaced carbon atom impacts will propagate efficiently along defect-free SWNTs owing to their high thermal conductivity, and so will be 'targeted' at barriers along the thermal and electrical conduction paths: a build-up of temperature if heat flow is limited at the barrier could anneal away the barrier, allowing more heat flow to the next barrier along the tube. This scenario explains why the conductivity of the paper samples can be increased significantly even when the ions can penetrate only a very small fraction of the sample. A percolated portion of the sample with enhanced conductivity would significantly increase the total current through the sample. Because this heating effect spreads out quickly from the impact sites, a corresponding initial increase in conductivity is observed. The initial increase and then decrease of the fluctuation-assisted tunnelling term in Fig. 4b as dose increases strongly suggests that enhancement of the pre-existing tunnelling conductivity plays a key role in causing the initial increase in conductivity in Fig. 4a. Changes due to direct impact damage build up cumulatively as initially only a small fraction of nanotubes suffer impacts. Once most of the accessible small barriers are annealed, the heating increase will tend to saturate, while the ion impacts continue to affect more SWNTs as the dose

increases, leading to the decrease in conductivity at higher doses.

Our scenario is supported by the fact that the conductivity peak is less pronounced for irradiation by N^+ ions even though their energy is the same as that of the Ar^+ ions. The key difference is that the N^+ ions penetrate about 60% further into the sample, so the deposition of heat energy from collisions initially extends over a greater depth from the surface of the sample. Hence, the density of heat energy deposited in the sample by N^+ ions is smaller, and the initial temperature rise will therefore be less than that for the Ar^+-ion bombardment. These lower annealing temperatures for N^+ ions imply that the conductivity increase in our thermal annealing scenario would be predicted to be less. This is what we observe experimentally.

To test our scenario further, we have performed thermal annealing experiments on pristine samples and made a comparison with samples from the same SWNT paper after irradiation. In the thermal annealing experiment the whole of each sample is heated in a vacuum. As shown in Fig. 5, thermal annealing of a sample of low-conductivity free-standing SWNT paper gives an increase in conductivity similar to that of irradiation, supporting our conclusion that the initial increase of conductivity due to the irradiating ions is due not to the direct impact effect, but to propagation deeper into the sample of the heat produced by the ion impacts.

Further support for this scenario is provided by our measurements (Fig. 5) on a paper sample with enhanced initial conductivity of over 1000 S/cm that has fewer tunnelling barriers or other defects and a larger carrier density (this conductivity is comparable to some of our earlier samples with particular dopants [16]). In this case of initial high conductivity, the irradiation and thermal annealing again produce a qualitatively similar effect, but this time it is a decrease in conductivity. The decrease in this high-conductivity case corresponds to annealing away of dopants (electron acceptors) that cause high conductivity [16].

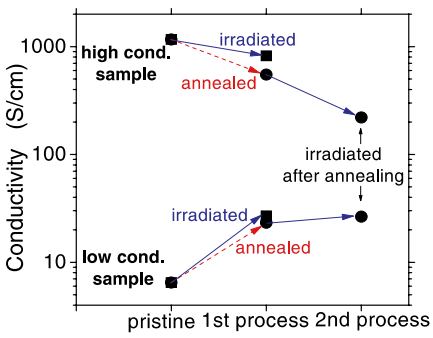

FIGURE 5 Comparison of the effect on low and high conductivity free-standing SWNT papers (thickness $\sim 50\,\mu m$) of Ar^+ irradiation with 10^{12} ions/cm^2, and of annealing at 500 °C for 1 h, followed by irradiation with the same dose

6 Conclusions

We have found that irradiation by ions (Ar^+ or N^+) modifies electronic conduction in SWNT networks in very different ways depending on their thickness. Our key conclusions for thin networks in which most ions pass through with only partial loss of energy are:

1. In the first measurements (to our knowledge) of ion irradiation of thin transparent SWNT networks, conductance is always reduced by the irradiation as the radiation damage localizes electron states at points along the SWNTs. The conductance follows variable-range hopping conductivity behaviour, with the faster decrease with temperature after ion irradiation indicating increased localization of the charge carriers (Fig. 3).
2. This reduction of conductance means that the operation of devices using thin SWNT films is likely to be affected by high-radiation environments. The fractional decrease in conductance is much larger at low temperatures than at room temperature, so devices using such thin SWNT networks would be much more sensitive to radiation damage when operating at low temperature than at room temperature.

For thicker networks (SWNT paper) in which all ions are stopped, our conclusions are:

4. We have discovered relatively sharp peaks of conductivity in SWNT paper as a function of irradiation dose (Fig. 2b). At high doses, irradiation of SWNT paper produces the expected gradual decrease in conductivity.
5. Combining a variety of measurements, we have concluded that the increase of conductivity produced by low doses of ion irradiation in most of our SWNT paper samples is due to removal of conduction barriers by heat propagated away from the impact region penetrated by the ions. We suggest that such thermal annealing causes an increase in conductivity that is initially larger than the decrease due to direct-impact damage, since the heat is quickly propagated along the SWNTs from the collision sites and anneals a larger volume of the sample than that affected by direct-impact damage.
6. It is therefore crucial in assessing the changes in the operation of devices exposed to ion irradiation to consider the sensitivity of the conduction properties not just to the direct-impact effects but also to heating effects in regions beyond the ions' penetration depth. This is also the case in using ion irradiation for nano-engineeering or modification of the properties of SWNT networks.
7. We have supported our interpretation of the origin of the conductivity peak by demonstrating a direct correlation between the effects of direct heating and ion irradiation on samples of different morphology: an initial increase of conductivity on irradiation and heating for moderately conducting SWNT paper, but a decrease of conductivity on both heating and irradiation for already highly conducting SWNT paper (Fig. 5).
8. We propose a simple model (3) that accounts very well for the behaviour of the temperature-dependent conductivity and provides a clear physical explanation of the observations. This model involves a parallel combination of metallic conduction along SWNTs interrupted by small tunnelling barriers, together with a hopping-type conduction term (as shown by the hopping and tunnelling terms in the fits in Fig. 4). The initial increase of the tunnelling term in Fig. 4b strongly suggests that enhancement of the pre-existing tunnelling conductivity plays a key role in the initial increase in conductivity. This type of model should be of wider use in modelling conduction in thicker SWNT networks where

only some layers of the sample are modified.

ACKNOWLEDGEMENTS This work was supported by EC project SANES and the Slovak national project APVV-0628-06. Z.O., G.V., and L.P.B. are grateful for financial support from the project OTKA grant T043685 and the NKTH grant MOFENACS.

REFERENCES

1 C. Gómez-Navarro, P.J. De Pablo, J. Gómez-Herrero, B. Biel, F.J. Garcia-Vidal, A. Rubio, F. Flores, Nat. Mater. **4**, 534 (2005)
2 B. Biel, F.J. Garcia-Vidal, A. Rubio, F. Flores, Phys. Rev. Lett. **95**, 266 801 (2005)
3 W.-K. Hong, C. Lee, D. Nepal, K.E. Geckeler, K. Shin, T. Lee, Nanotechnology **17**, 5675 (2006)
4 G. Gruner, J. Mater. Chem. **16**, 3533 (2006)
5 Y. Zhou, A. Gaur, S.-H. Hur, C. Kocabas, M.A. Meitl, M. Shim, J.A. Rogers, Nano Lett. **4**, 2031 (2004)
6 E.S. Snow, J.P. Novak, P.M. Campbell, D. Park, Appl. Phys. Lett. **82**, 2145 (2003)
7 J.X. Li, F. Banhart, Nano Lett. **4**, 1143 (2004)
8 A.V. Krasheninnikov, K. Nordlund, Nucl. Instrum. Methods Phys. Res. B **216**, 355 (2004)
9 M. Terrones, F. Banhart, N. Grobert, J.-C. Charlier, H. Terrones, P.M. Ajayan, Phys. Rev. Lett. **89**, 075 505 (2002)
10 A.V. Krasheninnikov, K. Nordlund, J. Keinonen, F. Banhart, Phys. Rev. B **66**, 245 403 (2002)
11 M. Terrones, P.M. Ajayan, F. Banhart, X. Blase, D.L. Carroll, J.-C. Charlier, R. Czerw, B. Foley, N. Grobert, R. Kamalakaran, P. Kohler-Redlich, M. Rühle, T. Seeger, H. Terrones, Appl. Phys. A **74**, 355 (2002)
12 H. Stahl, J. Appenzeller, R. Martel, P. Avouris, B. Lengeler, Phys. Rev. Lett. **85**, 5186 (2000)
13 Z. Osváth, G. Vértesy, L. Tapasztó, F. Wéber, Z.E. Horváth, J. Gyulai, L.P. Biró, Phys. Rev. B **72**, 045 429 (2005)
14 A.V. Krasheninnikov, K. Nordlund, M. Sirviö, E. Salonen, J. Keinonen, Phys. Rev. B **63**, 245 405 (2001)
15 M. Shiraishi, M. Ata, Synth. Met. **128**, 235 (2002)
16 V. Skákalová, A.B. Kaiser, U. Dettlaff-Weglikowska, K. Hrnčariková, S. Roth, J. Phys. Chem. B **109**, 7174 (2005)
17 V. Skákalová, A.B. Kaiser, Y.-S. Woo, S. Roth, Phys. Rev. B **74**, 085 403 (2006)
18 J.P. Biersack, L. Haggmark, Nucl. Instrum. Methods **174**, 257 (1980)
19 J.F. Ziegler, *The Stopping and Range of Ions in Matter*, vols. 2–6 (Pergamon, London, 1977–1985)
20 N.F. Mott, E.A. Davis, *Electronic Processes in Non-Crystalline Materials*, 2nd edn. (Clarendon, Oxford, 1979)
21 A.B. Kaiser, Rep. Prog. Phys. **64**, 1 (2001)
22 A.L. Efros, B.I. Shlovskii, J. Phys. C Solid State Phys. **8**, L49 (1975)
23 V. Skákalová, U. Dettlaff-Weglikowska, S. Roth, Diam. Relat. Mater. **13**, 296 (2004)
24 C. Mikó, M. Milas, J.W. Seo, R. Gaál, A. Kulik, L. Forró, Appl. Phys. Lett. **88**, 151 905 (2006)
25 C. Mikó, M. Milas, J.W. Seo, E. Couteau, N. Barisic, R. Gaál, L. Forró, Appl. Phys. Lett. **83**, 4622 (2003)
26 P. Sheng, Phys. Rev. B **21**, 2180 (1980)
27 Y. Woo, G. Duesberg, S. Roth, Nanotechnology **18**, 095 203 (2007)
28 S.P. Hepplestone, A.M. Ciavarella, C. Janke, G.P. Srivastava, Surf. Sci. **600**, 3633 (2006)